

Original Article

# Stress Localization in the Wide Cantilever Beams-A 2D Theory

Kaushal Kumar<sup>1</sup>, Gyani Jail Singh<sup>2</sup>

<sup>1,2</sup>Department of Civil Engineering, National Institute of Technology Patna, India.

<sup>1</sup>Corresponding Author : [kaushalk.phd19.ce@nitp.ac.in](mailto:kaushalk.phd19.ce@nitp.ac.in)

Received: 17 June 2022

Revised: 06 September 2022

Accepted: 21 October 2022

Published: 23 October 2022

**Abstract** - Based on the shear lag effect, stress localization has been studied in beams such as box beams, T-beams, and U-beams. A study of stress localization within a simple wide beam is presented using the energy principle. Conveniently, the close-form solutions of the differential equations are derived. Solving the differential equations, simple equations for bending stresses and deflections are presented considering the stress localization due to the shear lag effect. The methodology is illustrated by a numerical example demonstrating its simplicity and accuracy. The theoretical results are validated with literature and finite element analysis (FEA). The theoretical results are closely in line with the literature and FEA. Stress localization has reduced the bending moment capacity of the example beam by 30% for uniform distribution of the load (UDL) and 21% for point loads (PL). Short wide beams such as pier heads are highly recommended to consider stress localization, as this reduces the bending capacity of the beam.

**Keywords** - Shape function, Effective width, Stress localization, Warping, Wide beam.

## 1. Introduction

The wide cantilever beam is commonly used in engineering designs as cantilever walls, projecting floor slabs, projecting pier heads, and gear teeth. [1] Wide cantilever beams are also available as box-, U-, and I-beams. The thin cover plates as flanges in these structures are generally stiffened by an attached member called the web. Beams are used in ship hulls, floors, aircraft, bridges, and buildings. The stress distribution is not uniform across the width of this type of beam, like narrow beams. The assumption in elementary beam theory (EBT) is no longer valid for wide beams such as box beams because of the shear deformability of the flanges. [2] The effect is known as shear lag.

By preventing lateral deformation, thin metallic strips provide more rigidity. At wide beams' extreme edges, there is still a trace of the anticlastic curvature that exists primarily in narrow rectangular beams. In the meantime, the beam's central part maintains its flatness in the transverse direction. [3] Ashwell demonstrated that the stiffness of rectangular beams of moderate width depends not only upon the depth-width ratio of the beam but also upon the curvature to which the beam bends. [4] Deflection and stress distribution are not equal along the width of a very-short wide beam. [5-6] The effective width concept was brought in to calculate the strength of such beams. An effective width is the width of a transform beam cross section that gives the correct value of

maximum bending stress based on elementary beam theories. [7-9]

Additionally, the effective width depends on the type of support and loading, as well as the aspect ratio. [10] Studies have been conducted on analysing wide cantilever beams under concentrated loads and considering the stress concentrations under the load. [10-13] It is possible to solve the problem by applying thin-plate theory, either assuming an infinite plate width or applying it to a beam up to four times the span. In their article, Wellauer and Seireg demonstrate an empirical method for analyzing finite-width beams under arbitrary transverse loads and demonstrate that the previous analysis' assumption of a beam's infinite width is equally applicable to a beam of width as small as four times its span. [14] The bending of thin rectangular plates with various boundary conditions has been studied in the past. However, finding solutions satisfying a plate's partial differential equation and other boundary conditions is difficult. [15] Superposition is one of the methods used for exact bending solutions for thin plates. [16-18] Khalili et al. used Fourier series expansion to determine the precise bending of the plates. [19] A thin cantilever plate was analysed with a variety of numerical methods. Holl first analysed a thin cantilever wide beam using the finite difference method for a point load at a free end. [10]



Similarly, Barton, Neal, Livesley, and Birchall used the same method to solve the same problem separately. [20-22] Nash applied the approximate method to analyse the cantilever plate under uniform pressure. [23] Shu, Shih, and Plass et al. utilized the generalized variational principle to calculate the deflection of the thin rectangular plate. [24-25] A square cantilever plate was also loaded uniformly using the Rayleigh-Ritz and point matching techniques. [26]

The stress concentration problem is studied regarding shear lag in wide beams such as box beams, I-T-, and U-beams. The flange stress distribution corresponds to a 2D plane stress problem.[27-28] The cross-sections of wide beams such as box beams, U-T-, and I-beams used in engineering designs are not always flat. Shearing stresses cause it to warp. [3] It is well known that the warping restraints are located in support of the cantilever. Restraining the warping of the beam caused the stress concentration problem. As the flange is bound to the support of a cantilever beam and integrally stiffened by the web along its length in I-, T-, and U-beams, the warping is restrained in two ways. The restraining of free distortion resulted in unequal bending stress distribution. [29-32] As a result, stresses are most significant near the flange-web junction. [8]

Moreover, this case was noted as a positive shear lag. [2, 33-34] It is known as negative shear lag when actual stresses are lowest near the flange-web junction. [35-38] Various scholars analysed the shear lag effect describing the flange alone in the 2D model.[39-45] Numerous theories apply warping displacement functions to describe stress localisation as a shear lag effect. [42-45] Rovnak and Rovnakova reported that shear flow gradient and constraints on the flange warping caused the shear lag effect. [45]

The energy method has proven versatile among the methods reported by various scholars to analyse box-type structures. [28, 46-49] Concerning the energy method, the stress-compatibility equilibriums are included in the least work, and strain-compatibility equilibriums are used in the potential energy method. [2, 27 33, 35, 42-47] The shape function of the warping displacement in a box beam's cover sheet assumes polynomial variations. [2, 33, 35, 52, 54] Indirectly, the shape function for the warping indicates the stress distribution along the width of the beam. [31, 35, 49-52] Shear lag can therefore be viewed as a stress localization problem, represented mathematically by the effective width of the section.

An extensive literature review indicates that various novel methods are available for analysing wide cantilever beams with thin plates of infinite width, semi-infinite width, or other size cantilever beams as small as four times their spans. A few publications consider thin or moderately thick plate cantilevers with one or two span-to-width ratios. Using a thin cantilever plate, bending the cylindrical shape, and lifting two

free corners produce more complex boundary conditions. The higher stress concentration, and thus more significant deformation under the load, poses another problem to the analysis of thin cantilever plates. [3, 16] In the beams of web-flange arrangement, the part of the flanges at a distance from the web does not share fully in the resisting bending moment. Hence, the beam is weaker than the elementary bending theory suggests. [2, 29-31, 51] In these beams, the shear forces are transmitted to the flange adjoining the web during the bending. Thus, the stress distribution in the flange presents a 2D-stress problem.

For the same reason, the middle portion of a wide cantilever beam may become rigid, but the other part across the width may become weaker during bending. Stress localization will then occur in the centre line of the beam at the support and can be analysed in terms of shear lag. The present study considers thick cantilever plates with a finite width as a wide cantilever beam. In this case, the beam restrains free warping at the fixed end. In the present analysis, the shear deformation in the wide cantilever beam is considered an addition to the elementary beam theory. Thus, the study introduced a higher-order beam theory for simple wide beams incorporating additional boundary conditions.

## 2. Methodology

### 2.1. Analytical Formulation

A wide cantilever beam consisting of length  $l$ , width  $2w$ , and thickness  $t$  is considered in the present study. The spanwise coordinate is  $x$ , the perpendicular coordinates are  $y$  and  $z$ , and  $z(x)$  is the neutral deflection axis of the beam (Fig. 1). The following assumptions are incorporated

1. Stress concentration under load is ignored.
2. A uniform distribution of the load is assumed across the width.
3. The anticlastic deformation at the edges of the wide cantilever beam is ignored.
4. The corresponding spanwise displacement is

$$u(x, y) = \pm h \left( \frac{dz}{dx} + \frac{y^2}{w^2} U(x) \right) \quad (1)$$

Where,  $U(x)$  is a shear lag correction factor.

The potential energy of the beam for a bending moment  $M$  generated by a load system is

$$\Pi_l = \int M \frac{d^2z}{dx^2} dx \quad (2)$$

The strain energy of the beam is

$$\Pi_s = \frac{1}{2} \iiint \{ E \varepsilon_x^2 + G \gamma^2 \} dx dy dh \quad (3)$$

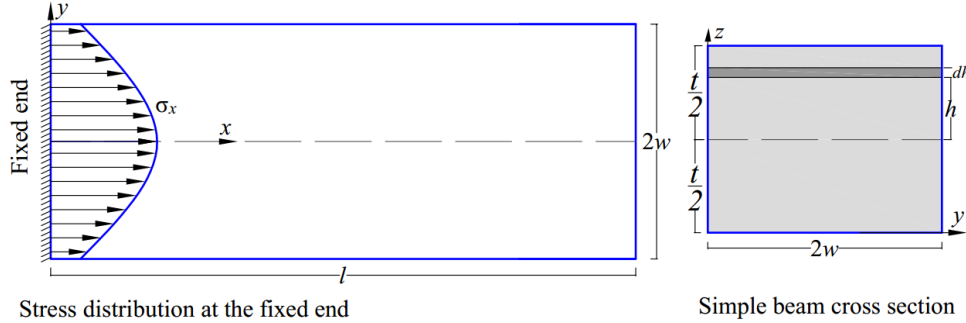


Fig. 1 Simple wide cantilever beam (geometry and coordinate system)

The spanwise linear strain and shear strain is obtained from Equation 1 as:

$$\epsilon_x = \pm h \left( z'' + \frac{y^2}{w^2} U' \right) \quad (4)$$

$$\gamma = \pm \frac{2h}{w} \frac{y}{w} U \quad (5)$$

Combining Equations 3, 4, and 5, the strain energy of the beam is

$$\Pi_s = \frac{1}{2} \iiint E h^2 \left\{ \left( z'' + \frac{y^2}{w^2} U' \right)^2 + \frac{G}{E} \left( \frac{2y}{w} U \right)^2 \right\} dx dy dh \quad (6)$$

After integrating Equation 6 and arranging the terms, the strain energy is

$$\Pi_s = \frac{1}{2} \int EI \left\{ (z'')^2 + \frac{1}{5} (U')^2 + \frac{2}{3} z'' U' + \frac{G}{E} \frac{4}{3w^2} U^2 \right\} dx \quad (7)$$

Where  $I = wt^3/6$

After combining Equations 2 and 7, the sum of the potential energy  $\Pi_T$  for the beam is

$$\Pi_T = \int \left\{ \frac{1}{2} EI (z'')^2 + M z'' \right\} dx + \int \frac{1}{2} EI \left\{ \frac{1}{5} (U')^2 + \frac{2}{3} z'' U' + \frac{G}{E} \frac{4}{3w^2} U^2 \right\} dx \quad (8)$$

Considering the interval of integration as  $x_1$  and  $x_2$  and applying the minimum potential energy principle from Equation 8

$$\delta \Pi_T = \int \left\{ \left[ EI (z'')^2 + M z'' + \frac{1}{3} EI U' \right] \delta z' + EI \left[ -\frac{1}{5} (U')^2 - \frac{1}{3} z'' + \frac{G}{E} \frac{4}{3w^2} U \right] \delta U \right\} dx + \left\{ EI \left[ \frac{1}{5} U' + \frac{1}{3} z'' \right] \delta U \right\}_{x_1}^{x_2} \quad (9)$$

From the variational method, making  $\delta \Pi_T = 0$ , the following relations can be established.

$$z'' + \frac{U'}{3} + \frac{M}{EI} = 0 \quad (10)$$

$$EI \left[ U'' - \frac{20G}{3E} \frac{1}{w^2} U + \frac{5}{3} z'' \right] = 0 \quad (11)$$

$$\left\{ EI \left[ \frac{1}{5} U' + \frac{1}{3} z'' \right] \delta U \right\}_{x_1}^{x_2} = 0 \quad (12)$$

From Equations 10 and 11

$$z'' - \frac{w^2 E}{15 G} z^{iv} = -\frac{M}{EI} + \frac{3w^2 E M''}{20 G EI} \quad (13)$$

On comparing Equation 13 with the Reissner [2], one of the Reissner parameters,  $n$ , become constant in this case, and the other parameter,  $k$ , is derived as:

$$k = \frac{1}{w} \sqrt{15 \frac{G}{E}} \quad (14)$$

Now, Equation 13 can be arranged as

$$z'' - \frac{z^{iv}}{k^2} = -\frac{M}{EI} + \frac{9}{4k^2} \frac{M''}{EI} \quad (15)$$

From Equations 1 and 10, the equation of the bending stress

$$\sigma_x = \pm E h \left[ \frac{M}{EI} + \left( \frac{1}{3} - \frac{y^2}{w^2} \right) U' \right] \quad (16)$$

## 2.2. Closed-Form Solutions

If the origin is at the cantilevers' free end, the fixed end has co-ordinate  $x = l$ . The cantilever beam is analyzed for UDL and PL. The load intensity and its position are depicted in the figures presented subsequently. The close-form solutions for the bending stresses for the individual load cases can be derived by closely following Reissner [2], Singh et al. [55], and Kumar and Singh [59]. The equations for the bending stress distribution in the cantilever beam for UDL and PL is shown in Equation 17 and 18, respectively.

$$\sigma(x, y) = \pm \frac{ql^2 h}{2 I} \left[ \left( \frac{x}{l} \right)^2 + \left( \frac{1}{3} - \frac{y^2}{w^2} \right) \frac{15}{2} \frac{1}{(kl)^2} \frac{\cosh k(l-x) + kl \sinh kx}{\cosh kl} - 1 \right] \quad (17)$$

$$\sigma(x, y) = \pm Pl \frac{h}{I} \left[ \frac{x}{l} + \left( \frac{1}{3} - \frac{y^2}{w^2} \right) \frac{15}{4} \frac{1}{kl} \frac{\sinh kx}{\cosh kl} \right] \quad (18)$$

$$z(x) = \frac{ql^4}{8EI} \left[ \frac{1}{3} \left( \frac{x}{l} \right)^4 - \frac{4}{3} \left( \frac{x}{l} \right) + 1 + \frac{10}{(kl)^2} \left\{ \frac{1}{2} \left( 1 - \left( \frac{x}{l} \right)^2 \right) + \frac{\cosh kx - \cosh kl}{(kl)^2} - \frac{\sinh kx - \sinh kl}{(kl)^2 \cosh kl} (\sinh kl - kl) \right\} \right] \quad (19)$$

$$z(x) = \frac{Pl^3}{3EI} \left[ \frac{1}{2} \left( \frac{x}{l} \right)^3 - \frac{3}{2} \left( \frac{x}{l} \right) + 1 + \frac{15}{4(kl)^2} \left\{ -\frac{x}{l} + 1 + \frac{\sinh kx}{kl \cosh kl} - \frac{\tanh kl}{kl} \right\} \right] \quad (20)$$

Additionally, the deflection of the beam can be obtained by integrating Equation 10 twice after eliminating  $U'$  and putting the values of  $M$  in it. The integral constants are determined by applying the boundary conditions: at  $x = l$ ,  $z(x)$ , and  $z'(x)$  equals zero. Thus, the deflection equation of the beam for UDL and PL are derived as shown in Equations 19 and 20, respectively.

### 3. Results and Discussion

#### 3.1. Validation of the Methodology

The beam's cross-section is obtained by transforming the box beam cross-section to validate the methodology (Fig. 2). The present study considers length of the box beam  $l = 125$  mm, width  $2w = 50$  mm, web and flange thickness  $t_w = t_f = 5$  mm, and depth = 50 mm. The box beam cross-section has  $I = 307500$  mm<sup>2</sup>. Furthermore, the box beam cross-section is transformed into a simple wide beam of solid cross-section having the same cross-sectional width, i.e.,  $2w = 50$  mm, and the principal moment of inertia ( $I$ ). The transform thickness is calculated as  $t = 41.94551$  mm  $\approx$  41.95 mm. The transformed simple wide cantilever beam of a solid cross section is utilized as an example in the present paper. The other geometrical property, and material properties for both beam is as: aspect ratio  $l/w = 5$ ,  $E = 200$  GPa,  $\mu$  (Poisson's ratio) = 0.3,  $G = 1000/13$  GPa, and  $G/E = 5/13$ .

A 3D-finite-element model of the wide beam was developed with ANSYS 15 software. Applying  $u(x) = u(z) = 0$  produced the boundary condition of the cantilever at the support. The model was analyzed using a 20-noded (SOLID186) element.

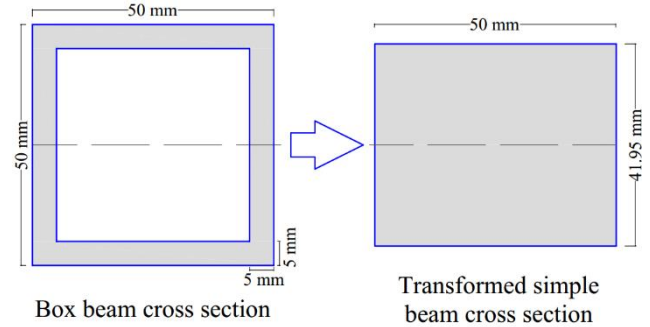


Fig. 2 Beam cross-sections

The mesh convergence study minimizes errors and computer run time [61]. The model was discretized by dividing it into 13, 5, and 5 divisions in the x-direction, y-direction, and z-direction resulting in a total of 325 elements (Fig. 3).

The deflection profiles for the wide cantilever beam derived from Equations 19 and 20 are closely matched with those from FEA, box beam, and elementary beam theory (EBT) (Fig. 4). It is evident from Fig. 4 that the shear lag effect increased the deflection of the wide cantilever beam compared to the Euler-Bernoulli beam. As a result of the additional shear deformation caused by the shear lag in the beam, the maximum deflection for UDL and PL is increased by approximately 2.9 and 2.6 %, respectively, compared with the Euler-Bernoulli beam. In this way, the shear lag observed to be added to the deflection of the wide cantilever beam is similar to that of the cantilever box beam. However, the maximum deflection of the wide beam is considerably less than the box beam. It is observed that the added deformation is lower for wide cantilever beams than for box beams because they have a higher stiffness.

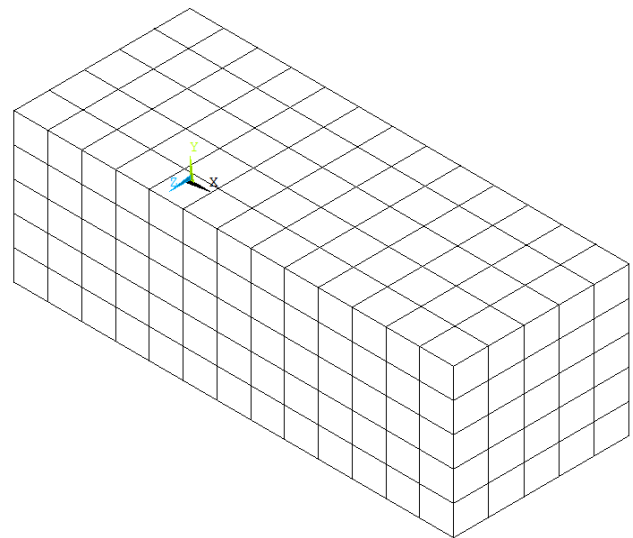


Fig. 3 FE model for the wide beam

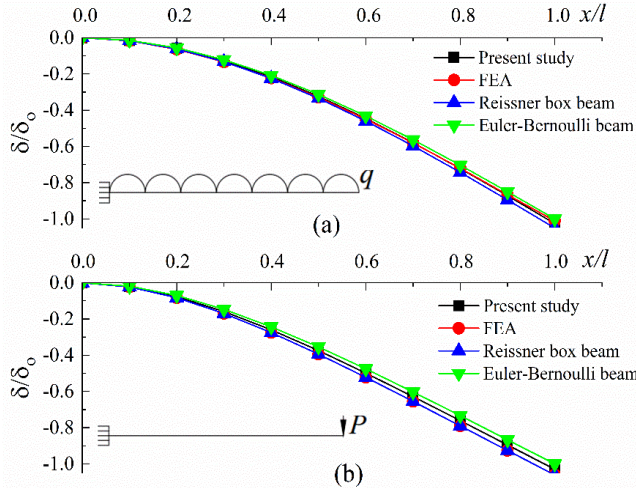


Fig. 4 Deflection profile for wide beam: (a) UDL and (b) PL

Additionally, Fig. 5 demonstrated the robustness of the methodology as the stresses in the center line at the top fiber of the beam throughout the length are compared with those obtained by FEA. The results of the FEA are in excellent agreement with the theoretical development, except for some deviations near the fixed end caused by FEA singularities. [61]

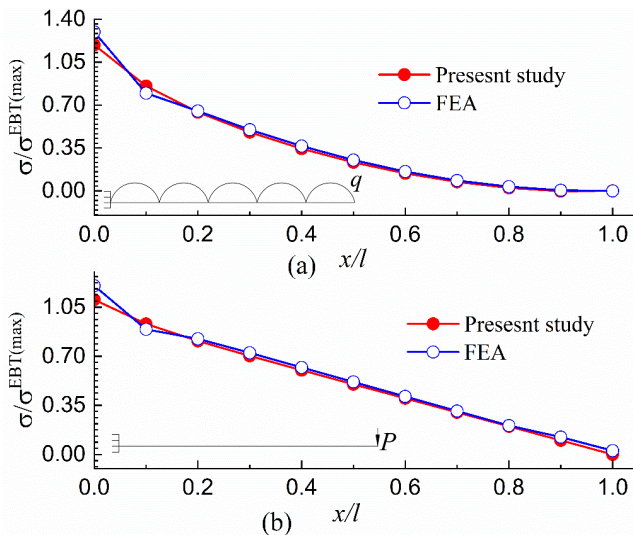


Fig. 5 Comparing the stresses in the center line at the top fiber of the beam along the length: (a) UDL and (b) PL

### 3.2. Applications

The wide cantilever beam considered in this study produces localized stress in the central line at its fixed end. The additional deformation caused by the shear lag effect increases the stresses in the center line of the beam at the support. Accordingly, the center region of the wide cantilever beam is stiffer than the rest of the beam. Thus, calculating the stress by EBT will lead to some severe errors in a wide beam. The transmission of the shear is reversed to those of the box cantilever beam [2], and therefore the shear deformation results from the stress concentration in the center of the beam

at the support. To measure the stress localization, the effective width ratio ( $b_e$ ) can be calculated using the formulae shown in Equation 21 [49].

$$b_e = \frac{1}{w} \left[ \frac{1}{\sigma_{max}} \int_0^w \sigma dy \right] \quad (21)$$

The effective width ratio for the uniformly distributed and point loads is calculated in the present study as follows.

$$b_{e(UDL)} = \frac{1}{1 + \frac{5}{2} \frac{1}{(kl)^2} (kl \tanh kl - 1)} \quad (22)$$

$$b_{e(PL)} = \frac{1}{1 + \frac{5 \tanh kl}{4 kl}} \quad (23)$$

For a wide beam of length equal to width, i.e.,  $l/w = 2$ ,  $b_e$  is 0.708 for UDL and 0.794 for PL. However,  $b_e$  of the box beam consisting of the same material property, the moment of area and aspect ratio (Fig. 2) were calculated and found to be 0.519 and 0.612 for UDL and PL, respectively.  $b_e$  of the cantilever box beam was lower than the wide cantilever beam. The higher shear deformation in the flange of the box beam resulted in higher stress concentration at the web-flange junction and thus produced higher deflection and lowered effective width.

Even though the wide cantilever beam was found to be more rigid than the box beam and to have a higher  $b_e$ , the stress localization in the center line at the fixed end reduced the effective width significantly. Accordingly, the example beam's bending moment capacity is reduced by around 30% and 21% in the case of UDL and PL, respectively. Pier heads are typically designed for point loading. The column head should be designed for 1.26 times the design bending moment in the present case. The following sections explain how the other parameter affects the effective width ratio of the wide cantilever beam.

### 3.3. Parametric Analysis

Lowering the aspect ratio ( $l/w$ ) severely influenced the  $b_e$ . The aspect ratio is higher for narrow beams and lowers for wide beams. The other parameter that may influence the  $b_e$  is the material properties ( $G/E$  ratio). The influence of these two parameters on  $b_e$  is presented in the subsequent paragraph.

#### 3.3.1. Effect Of Aspect Ratio

Fig. 6, which displays the variation of  $b_e$  corresponding to aspect ratios, illustrates the importance of this parameter. Effective width ratios reach their highest values for narrow beams, i.e., for high aspect ratios. According to Moffatt and Dowling [49], stress localization is more pronounced for low aspect ratios. The effective width calculated for the PL is higher than the effective width calculated for the UDL. The rate variation in the effective width ratio for lower aspect ratios is higher for PL than for

UDL (Figure 6). Pier's heads are generally designed for a point load. If the aspect ratio is much lower, equal to 1 or 1/2, the effective ratio may be highly reduced in this case.

3.3.2. Effect of G/E Ratio

Fig. 7 shows the variation in the  $b_e$  concerning the variation in the G/E ratio in a wide cantilever beam for aspect ratio five. When the G/E ratio is higher, the  $b_e$  is more significant. For the G/E ratios of 0.18 and 0.65 and the aspect ratio of five, the  $b_e$  is 0.789, 0.868, and 0.870, 0.926 for UDL and PL, respectively.

As a result, the  $b_e$  increases as the G/E ratio increases. Additionally, the G/E ratio is much lower in the nonlinear deformation range, and the effective width ratio may be significantly reduced in these cases.

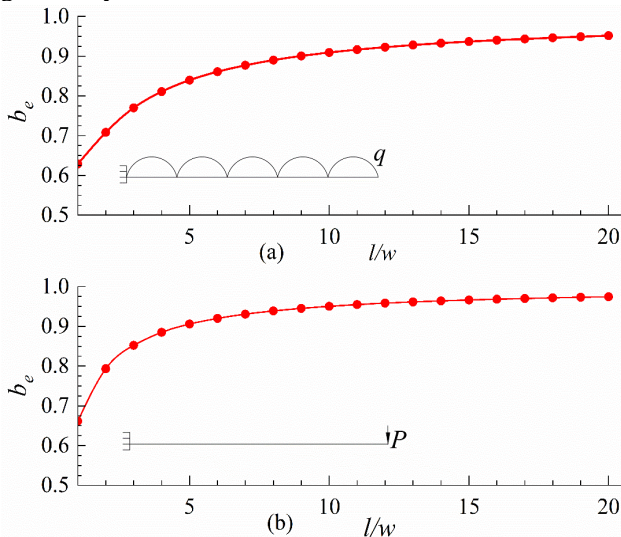


Fig. 6 Variation of  $b_e$  corresponding to  $l/w$  for: (a) UDL and (b) PL

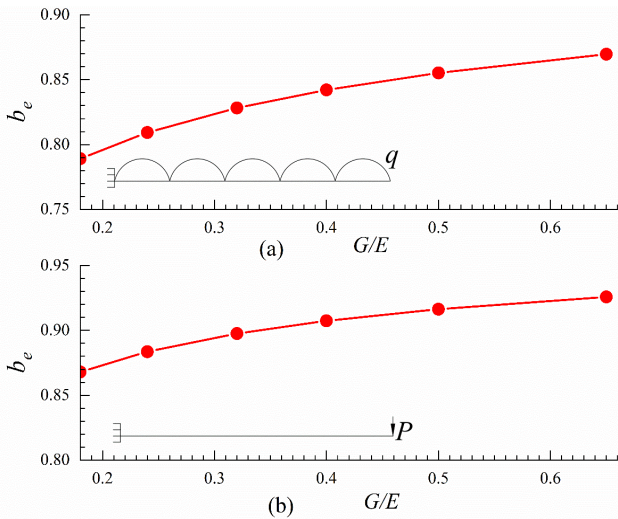


Fig. 7 Variation of  $b_e$  corresponding to G/E ratio for (a) UDL and (b) PL

4. Conclusion

The current study presents a simplified procedure to analyze the wide cantilever beam under shear loadings. The simple assumptions derive the simplified closed-form solution of the bending stresses and deflections. The methodology is illustrated by a numerical example demonstrating its simplicity and accuracy. The theoretical results are closely in line with the literature and FEA. As a result, the following conclusions are drawn.

It was observed that the stress was localized in the center line of the wide cantilever beam at the support. The wide cantilever beam was more rigid in its center line than any other part of the beam. Therefore, the stress localization in the beam significantly reduced its effective width.

The aspect ratio is a critical factor affecting the effective width. Lower aspect ratios result in increased stress concentration. For uniformly distributed and point loads, the effective width for aspect ratio two was 0.708 and 0.794, respectively.

This paper attempts to investigate stress localization by analyzing the wide cantilever beam. When considering the stress concentration due to the shear lag effect, the reduced effective width ratio or bending moment capacity of the wide beam, such as pier heads, must be considered in the design.

Appendix 1: Symbols

The symbols used are

- $E, G$  = Young's modulus and Shear modulus of beam
- $EI$  = Flexural rigidity of the cross section
- $h$  = Height of the fiber from neutral axis
- $I$  = Moment of inertia of beam cross section
- $\kappa, n$  = Reissner's parameters
- $l$  = Span length
- $M(x), M$  = Bending moment
- $P, q$  = Loadings intensity
- $t$  = Beam thickness
- $t_f, t_w$  = Thickness of flange and web
- $u(x)$  = Longitudinal displacement
- $u(z)$  = Vertical displacement
- $u(x, y)$  = Span wise sheet displacement
- $U(x)$  or  $U$  = Correction due to shear lag
- $w$  = Half width of the beam
- $x, y, z$  = Coordinates
- $x_1, x_2$  = End of the interval of integration
- $\delta$  = Deflection
- $\delta_0$  = Maximum deflection in EBT
- $\mu$  = Poisson's ratio
- $\epsilon_x, \gamma$  = Linear and shear strain of the cover sheet
- $\Pi_1, \Pi_2, \Pi_T$  = Potential energy
- $\sigma, \sigma_x, \sigma(x, y)$  = Bending Stress
- $\sigma_{max}$  = Maximum bending stress at the fixed end
- $\Delta\sigma$  = Additional bending stress
- $\sigma_{EBT}$  = Bending stress in EBT
- $\sigma^{EBT(max)}$  = Maximum bending stress in EBT (at the fixed end)

## References

- [1] W. C. Young, R. G. Budynas, “*Roark’s Formulas for Stress and Strain*,” 7th ed., McGraw-Hill, New York, 2002.
- [2] E. Reissner, “Analysis of Shear Lag in Box Beams by the Principle of Minimum Potential Energy,” *Quarterly of Applied Mathematics*, vol. 4, no. 3, pp. 268–278, 1946.
- [3] S. P. Timoshenko, J. N. Goodier, “*Theory of Elasticity*,” 3rd ed., McGraw-Hill, India, 2010.
- [4] D. G. Ashwell, “The Anticlastic Curvature of Rectangular Beams and Plates,” *J. R. Aeron. Soc.*, 54, 1950.
- [5] E. F. Kelley, “Effective Width of Concrete Bridge Slabs Supporting Concentrated Loads,” *Public Roads* (United States Department of Agriculture, Bureau of Public Roads), vol. 1, no. 7, 1926.
- [6] C. T. Morris, “*Concentrated Loads on Slabs*,” The Ohio State University College of Engineering (Sta Bull), vol. 80, 1933.
- [7] G. Winter, “Stress Distribution in and Equivalent Width of Flanges of Wide Thin-Wall Steel Beams,” *National Advisory Committee for Aeronautics Techology*, Note, vol. 784, 1940.
- [8] F. B. Hildebrand, E. Reissner, “Least-Work Analysis of the Problem of Shear Lag in Box Beams,” *National Advisory Committee for Aeronautics Techology*, Note, vol. 893, 1943.
- [9] A. Gjelsvik, “Analog-Beam Method for Determining Shear-Lag Effects,” *Journal of Engineering Mechanics*, vol. 117, no. 7, pp. 1575–94, 1991.
- [10] T. J. Jaramillo, “Deflections and Moments Due to a Concentrated Load on a Cantilever Plate of Infinite Length,” *Journal of Applied Mechanics*, vol. 17, no. 1, 1950.
- [11] N. C. Small, “Bending of a Cantilever Plate Supported from an Elastic Half Space,” *Journal of Applied Mechanics*, vol. 28, no. 3, pp. 387–94, 1961.
- [12] E. J. Wellauer, A. Seireg, “Bending Strength of Gear Teeth by Cantilever-Plate Theory,” *Journal of Engineering for Industry*, vol. 82, no. 3, pp. 213–20, 1960.
- [13] C. Li, B. Li, C. Wei, J. Zhang, “3-Bar Simulation-Transfer Matrix Method for Shear Lag Analysis,” *Procedia Engineering*, vol. 12, pp. 21–26, 2011.
- [14] S. P. Timoshenko, S. W. Krieger, “*Theory of Plates and Shells*,” 2nd ed., McGraw-Hill, India, 2010.
- [15] M. K. Huang, H. D. Conway, “Bending of a Uniformly Loaded Rectangular Plate with Two Adjacent Edges Clamped and the Others Either Simply Supported or Free,” *Journal of Applied Mechanics*, pp. 451–60, 1952.
- [16] F. V. Chang, “Bending of Uniformly Cantilever Rectangular Plates,” *Applied Mathematics and Mechanics*, vol. 1, pp. 371–383, 1980.
- [17] M. V. Barton, “*Finite Difference Equations for the Analysis of Thin Rectangular Plates with Combinations of Fixed and Free Edges*,” Defense Research Lab, Univ. of Texas, Rep. No. 175, 1948.
- [18] R. H. Mac Neal, “The Solution of Elastic Plate Problems by Electrical Analogies,” *Journal of Applied Mechanics*, pp. 59–67, 1951.
- [19] W. A. Nash, “Several Approximate Analyses of the Bending of a Rectangular Cantilever Plate by Uniform Normal Pressure,” *Journal of Applied Mechanics*, pp. 33–6, 1952.
- [20] T. K. Shu, T. T. Shih, “Variational Principle of Elastic Thin Plates and its Application,” *Journal of Beijing University of Aeronautics and Astronautics*, vol. 1, pp. 27–40, 1957.
- [21] H. J. Plass, J. H. Gaines, C. D. Newsom, “Application of Reissner’s Variational Principle to Cantilever Plate Deflection and Vibration Problems,” *The Journal of Applied Mechanics*, vol. 29, pp. 127–135, 1962.
- [22] A. W. Leissa, F. W. Nietenfuhr, “A Study of the Cantilevered Square Plate Subjected to a Uniform Loading,” *Journal of the Aerospace Sciences*, vol. 29, no. 2, pp. 162–169, 1962.
- [23] E. Reissner, “Least Work Solutions of Shear Lag Problems,” *Journal of the Aeronautical Sciences*, vol. 8, no. 7, pp. 284–91, 1941.
- [24] C. Meyer, A. C. Scordelis, “Analysis of Curved Folded Plate Structures,” *Journal of the Structural Division*, vol. 97, no. 10, pp. 2459–80, 1971.
- [25] H. R. Evans, N. E. Shanmugam, “Simplified Analysis for Cellular Structures,” *Journal of Structural Engineering*, vol. 110, no. 3, pp. 531–543, 1984.
- [26] Y. Okui, M. Nagai, “Block FEM for Time-Dependent Shear-Lag Behavior in Two I-Girder Composite Bridges,” *Journal of Bridge Engineering*, vol. 12, no. 1, pp. 72–79, 2007.
- [27] X. X. Qin, H. B. Liu, S. J. Wang, Z. H., Yan, “Simplistic Analysis of the Shear Lag Phenomenon in a t-Beam,” *Journal of Engineering Mechanics*, vol. 141, no. 5, pp. 1–15, 2015.
- [28] D. A. Foutch, P. C. Chang, “A Shear Lag Anomaly,” *Journal of Structural Engineering*, vol. 108, no. 7, pp. 1653–1658, 1982.
- [29] G. J. Singh, S. Mandal, R. Kumar, “Effect of Column Location on Plan of Multi-Story Building on Shear Lag Phenomenon,” *Proceedings of the of the 8th Asia-Pacific Conference on Wind Engineering (APCWE-VIII)*, Madras, India, pp. 978–981, 2013.
- [30] S. T. Chang, F. Z. Zheng, “Negative Shear Lag in Cantilever Box Girder with Constant Depth,” *Journal of Structural Engineering*, vol. 113, no. 1, pp. 20–35, 1987.
- [31] Q. Z. Luo, J. Tang, Q. S. Li, “Negative Shear Lag Effect in Box Girders with Varying Depth,” *Journal of Structural Engineering*, vol. 127, no. 10, pp. 1236–1239, 2001.

- [32] K. W. Shushkewich, "Negative Shear Lag Explained," *Journal of Structural Engineering*, vol. 117, no. 11, pp. 3543–3546, 1991.
- [33] Y. Singh, A. K. Nagpal, "Negative Shear Lag in Framed-Tube Buildings," *Journal of Structural Engineering*, vol. 120, no. 11, pp. 3105–21, 1994.
- [34] W. Yao, H. Yang, "Hamiltonian System-Based Saint Venant Solutions for Multi-Layered Composite Plane Anisotropic Plates," *International Journal of Solids and Structures*, vol. 38, no. 32–33, pp. 5807–5817, 2001.
- [35] L. Zhao, W. Chen, "Plane Analysis for Functionally Graded Magneto-Electro-Elastic Materials via the Simplistic Framework," *Composite Structures*, vol. 92, no. 7, pp. 1753–1761, 2010.
- [36] S. B. Dong, C. Alpdogan, E. Taciroglu, "Much Ado About Shear Correction Factors in Timoshenko Beam Theory," *International Journal of Solids and Structures*, vol. 47, no. 13, pp. 1651–65, 2010.
- [37] C. W. Liu, E. Taciroglu, "A Semi-Analytic Meshfree Method for Almansi–Michell Problems of Piezoelectric Cylinders," *International Journal of Solids and Structures*, vol. 45, no. 9, pp. 2379–2398, 2008.
- [38] V. Křístek and J. Studnička, "Negative Shear Lag in Flanges of Plated Structures," *Journal of Structural Engineering*, vol. 117, no. 12, pp. 3553–69, 1991.
- [39] M. Rovňák and L. Rovňáková, "Discussion on Negative Shear Lag in Framed-Tube Buildings," *Journal of Structural Engineering*, vol. 122, no. 6, pp. 711–713, 1996.
- [40] L. Zhu, J. Nie, F. Li, W. Ji., "Simplified Analysis Method Accounting for Shear Lag Effect of Steel-Concrete Composite Decks," *Journal of Constructional Steel Research*, vol. 115, pp. 62–80, 2015.
- [41] M. S. Cheung, Y. K. Cheung, "Analysis of Curved Box Girder Bridges by the Finite-Strip Method," *International Association for Bridges and Structural Engineering*, vol. 31, no. 1, pp. 1-8, 1971.
- [42] K. R. Moffatt, P. J. Dowling, "Shear Lag in Steel Box Girder Bridges," *Structural Engineers*, vol. 53, no. 10, pp. 439–448, 1975.
- [43] Z. Lin, J. Zhao, "Least Work Solutions of Flange Normal Stresses in Thin Walled Flexural Members with High Order Polynomials," *Engineering Structures*, vol. 33, no. 10, pp. 2754–2761, 2011.
- [44] P. C. Chang, "Analytical Modeling of Tube-in-Tube Structure," *Journal of Structural Engineering*, vol. 111, no. 6, pp. 1326–1337, 1984.
- [45] Z. Lin, J. Zhao, "Revisit of AASHTO Effective Flange-Width Provisions for Box Girders," *Journal of Bridge Engineering*, vol. 16, no. 6, pp. 881–889, 2011.
- [46] R. Mahjoub, R. Rahgozar, H. Saffari, "Simple Method for Analysis of Tube Frame by Consideration of Negative Shear Lag," *Australian Journal of Basic and Applied Sciences*, vol. 5, no. 3, pp. 309–316, 2011.
- [47] G. J. Singh, S. Mandal, R. Kumar, R. Kumar, "Simplified Analysis of Negative Shear Lag in Laminated Composite Cantilever Beam," *Journal of Aerospace Engineering*, vol. 33, no. 1, pp. 1-11, 2020.
- [48] Y. H. Zhang, L. X. Lin, "Shear Lag Analysis of Thin-Walled Box Girders Adopting Additional Deflection as Generalized Displacement," *Journal of Structural Engineering*, vol. 61, no. 4, pp. 73–83, 2014.
- [49] Q. Z. Luo, Q. S. Li, "Shear Lag of Thin-Walled Curved Box Girder Bridges," *Journal of Engineering Mechanics*, vol. 126, no. 10, pp. 1111–1114, 2000.
- [50] Q. Z. Luo, J. Tang, Q. S. Li, "Shear Lag Analysis of Beam-Columns," *Engineering Structures*, vol. 25, no. 9, pp. 1131–1138, 2003.
- [51] K. Kumar, G. J. Singh, "Stress Concentration in Composite Cantilever Plates — Effect of Stiffeners and Remedy," *Journal of The Institution of Engineers : Series A*, 2022.
- [52] Q. Song, A. C. Scordelis, "Formulas for Shear-Lag Effect of T-, I-, and Box Beams," *Journal of Structural Engineering*, vol. 116, no. 5, pp. 1306-1318, 1990.
- [53] M. C. M., Bakker, T. Pekoz, "The Finite Element Method for Thin Walled Members-Basic Principles," *Thin Walled Structure*, vol. 41, no. 2–3, pp. 179–189, 2003.